Detecting Entanglement in Quantum Many-Body Systems via Permutation Moments

Zhenhuan Liu,[1] Yifan Tang,[1,2,3] Hao Dai,[1] Pengyu Liu,[1] Shu Chen,[1] and Xiongfeng Ma[1,*]
[1]Center for Quantum Information, Institute for Interdisciplinary Information Sciences, Tsinghua University, Beijing 100084, China
[2]Department of Mathematics and Computer Science, Freie Universität Berlin, 14195 Berlin, Germany
[3]Department of Physics, Freie Universität Berlin, 14195 Berlin, Germany

(Received 22 March 2022; accepted 15 November 2022; published 23 December 2022)

Multipartite entanglement plays an essential role in both quantum information science and many-body physics. Because of the exponentially large dimension and complex geometric structure of the state space, the detection of entanglement in many-body systems is extremely challenging in reality. Conventional means, like entanglement witness and entropy criterion, either highly depend on the prior knowledge of the studied systems or the detection capability is relatively weak. In this Letter, we propose a framework for designing multipartite entanglement criteria based on permutation moments, which have an effective implementation with either the generalized control-SWAP quantum circuits or the random unitary techniques. As an example, in the bipartite scenario, we develop an entanglement criterion that can detect bound entanglement and show strong detection capability in the multiqubit Ising model with a long-range XY Hamiltonian. In the multipartite case, the permutation-moment-based criteria can detect entangled states that are not detectable by any criteria extended from the bipartite case. Our framework also shows potential in entanglement quantification and entanglement structure detection.

DOI: 10.1103/PhysRevLett.129.260501

The past decades have witnessed great progress in understanding quantum entanglement [1]. To date, entanglement acts not only as the cornerstone of quantum information science, but also as a new perspective in many other fields, like quantum thermodynamics [2,3], condensed matter physics [4], and quantum gravity [5]. Especially in many-body physics, the dynamical behavior, scaling property, and spectral form of entanglement are key indicators to characterize different phases of the system [6,7].

As a resource that cannot be produced by local operations and classical communication, entangled k-partite states are those that cannot be written in a separable form, $\rho = \sum_i p_i \rho_1^i \otimes \cdots \otimes \rho_k^i$, where $p_i \geq 0$ satisfies the normalization condition $\sum_i p_i = 1$ and ρ_r^i is the density matrix of the rth subsystem. As the dimension of a quantum system grows exponentially with the number of qubits, the geometric structure of state space becomes highly complicated, making entanglement detection a resource-consuming task. In fact, determining whether a state is entangled or not is generally a NP-hard problem [8]. For pure states or states with enough prior knowledge, entanglement can be effectively detected by purity measurements [3,9], variational algorithms [10], or entanglement witness [11,12]. While in the noisy intermediate-scale quantum era [13], the processed states are usually disturbed by unpredictable noise, rendering the detection capability of conventional means ineffective. Consequently, it is important to find implementable and efficient methods to detect multipartite entanglement with state-of-the-art devices.

For a generic mixed multipartite state without prior knowledge, there are two commonly used techniques to detect entanglement: density matrix moments and index permutation. Moments of density matrix, $\mathrm{tr}(\rho^n)$, carry much information about the states and are relatively easy to measure [14–16]. Hence, they become practical tools in estimating properties of quantum systems [17], including quantum entanglement [11,18–21]. However, most moment-based entanglement criteria are specially designed for states with few parties or low dimensions. A general moment-based entanglement-detection framework for multipartite systems is still missing.

Based on the rearrangement of density matrix elements, the index permutation criterion [22] can be applied in systems with an arbitrary number of parties and dimensions and has many generalizations [23]. In general, a k-partite quantum state can be represented using a matrix with $2k$ indices,

$$\rho = \sum_{s_1,\ldots,s_{2k}} \rho_{s_1 s_2,\ldots,s_{2k-1}s_{2k}} |s_1 \cdots s_{2k-1}\rangle\langle s_2 \cdots s_{2k}|, \quad (1)$$

where $s_1, s_3, \ldots, s_{2k-1}$ represent the row indices, and $s_2, s_4, \ldots, s_{2k}$ represent the column ones. The two indices, s_{2r-1} and s_{2r}, denote for the rth subsystem. By changing the order of these $2k$ indices, one gets a new matrix, $\mathcal{R}_\pi(\rho)$, with

$$[\mathcal{R}_\pi(\rho)]_{s_1 s_2,\ldots,s_{2k-1}s_{2k}} = \rho_{s_{\pi(1)}s_{\pi(2)},\ldots,s_{\pi(2k-1)}s_{\pi(2k)}}, \quad (2)$$

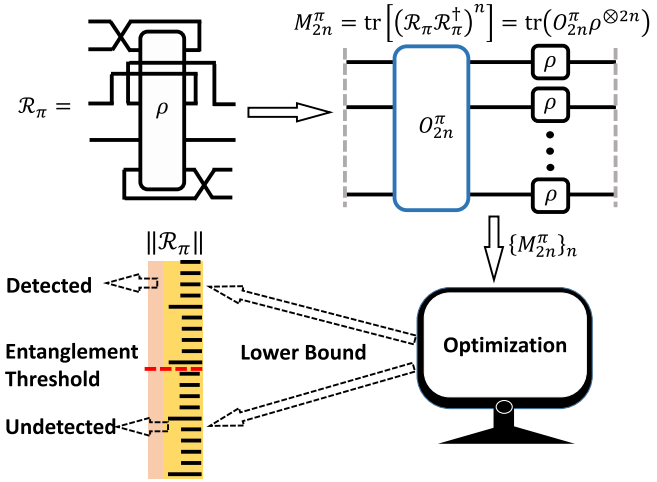

FIG. 1. Flowchart of entanglement detection. To detect multipartite entanglement of ρ, one needs to first choose an index permutation operation $\mathcal{R}_\pi(\cdot)$ and set $\|\mathcal{R}_\pi(\rho)\| = \sum_i \lambda_i$ as the entanglement indicator. Then, one measures the permutation moments $\{M_{2n}^{\pi} = \sum_i \lambda_i^{2n}\}_n$ and uses these moments to lower bound $\|\mathcal{R}_\pi(\rho)\|$. If the lower bound is larger than the entanglement threshold set for $\|\mathcal{R}_\pi(\rho)\|$, the multipartite entanglement is successfully detected. Otherwise, one can measure higher-order moments or pick another index permutation and repeat the procedure.

where π is an element of $2k$th permutation group $\mathcal{S}_{2k}$. For simplicity, hereafter, we use $\mathcal{R}_\pi$ to denote $\mathcal{R}_\pi(\rho)$. Using the property of index permutation, one could prove that [22]

$$\|\mathcal{R}_\pi\| = \mathrm{tr}\left(\sqrt{\mathcal{R}_\pi \mathcal{R}_\pi^\dagger}\right) = \sum_i \lambda_i \le 1, \tag{3}$$

for all k-partite separable states, where $\{\lambda_i\}$ are the singular values of $\mathcal{R}_\pi$. The violation of this inequality indicates entanglement. In the bipartite scenario, when setting π to be (1,2) and (2,3), where $(\cdot,\cdot)$ denotes exchanging two indices, one gets the widely used positive partial transposition (PPT) criterion [24] and the computable cross norm (CCNR) criterion [25], respectively. However, because index permutation is an unphysical operation, and the permutation criteria are based on singular value decomposition, a highly nonlinear operation, measurement of $\|\mathcal{R}_\pi\|$ usually requires full state tomography, which is extremely resource-consuming [26].

To harness the power of permutation criteria in multipartite entanglement detection, we borrow the idea from moment criteria. Although it is generally hard to measure $\|\mathcal{R}_\pi\|$ directly, one can alternatively estimate the higher-order moments, $M_{2n}^{\pi} = \mathrm{tr}[(\mathcal{R}_\pi \mathcal{R}_\pi^\dagger)^n] = \sum_i \lambda_i^{2n}$, which are much easier to access. These permutation moments can help to lower bound $\|\mathcal{R}_\pi\| = \sum_i \lambda_i$ and infer whether the state is multipartite entangled or not. A similar idea has also been used in the estimation of quantum negativity [27,28] and entropy [17]. By changing the index permutation operation $\mathcal{R}_\pi(\cdot)$ and measuring different orders of moments, we generate a series of implementable multipartite entanglement criteria, which we call "moment-based permutation criteria." The entanglement detection flowchart is shown in Fig. 1.

TABLE I. We use the tensor network to illustrate the four kinds of parties and their second and fourth moments. The boxes represent the subsystems of a generic k-partite state, and the two legs represent the row and column indices. The gray dashed lines represent periodic boundary condition. From the second line, one can find that the operators to estimate the second moments for all these four kinds of parties are the SWAP operators, which are represented by changing the order of two legs. Hence, $\mathrm{tr}(\mathcal{R}_\pi \mathcal{R}_\pi^\dagger) = \mathrm{tr}(\rho^2)$ for all $\pi \in \mathcal{S}_{2k}$. From the third line, one can find that the operators to estimate $\mathrm{tr}[(\mathcal{R}_\pi \mathcal{R}_\pi^\dagger)^2]$ for R-type parties are still SWAP operators, while the operators for T-type parties are cyclic permutation operators, which are represented by changing the order of the four legs cyclically.

Type	T1	T2	R1	R2
$\mathcal{R}_\pi$				
$\mathrm{tr}(\mathcal{R}_\pi \mathcal{R}_\pi^\dagger)$	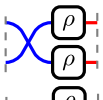	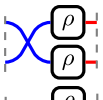	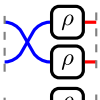	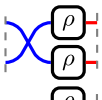
$\mathrm{tr}[(\mathcal{R}_\pi \mathcal{R}_\pi^\dagger)^2]$	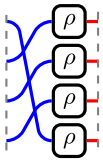	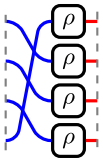	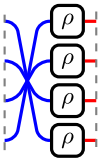	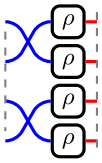

Moment-based permutation criteria.—For multipartite quantum state ρ, each party has two indices, one for row and one for column. Given $\mathcal{R}_\pi$, all the parties can be divided into four types based on the position transition of their two indices, as shown in the first line of Table I.

We find two properties of index permutation. First, if a party is T1 type or T2 type for $\mathcal{R}_\pi$, then it will keep the type for $\mathcal{R}_\pi^\dagger$; while if it is R1 type or R2 type for $\mathcal{R}_\pi$, then it becomes R2 type or R1 type for $\mathcal{R}_\pi^\dagger$, respectively. Second, the indices contraction in $M_{2n}^{\pi} = \mathrm{tr}[(\mathcal{R}_\pi \mathcal{R}_\pi^\dagger)^n]$ only acts on the indices from the same party of the $2n$ copies of ρ. Hence, if we list these $2n$ copies of states in order, the indices from an R-type party will contract with one of its two neighboring states and the indices from a T-type party will contract with both of its neighboring states. Note that $\mathcal{R}_\pi$ might not be a square matrix, so its odd moments are generally inaccessible.

Based on these results, we can prove that M_{2n}^{π} can be measured directly by a joint observable.

Theorem 1: Given a k-partite state ρ and the index permutation operation $\mathcal{R}_\pi$, the $2n$th moment of $\mathcal{R}_\pi$, $M_{2n}^{\pi} := \mathrm{tr}[(\mathcal{R}_\pi \mathcal{R}_\pi^\dagger)^n]$, can be estimated by observable measurement on $2n$ copies of ρ,

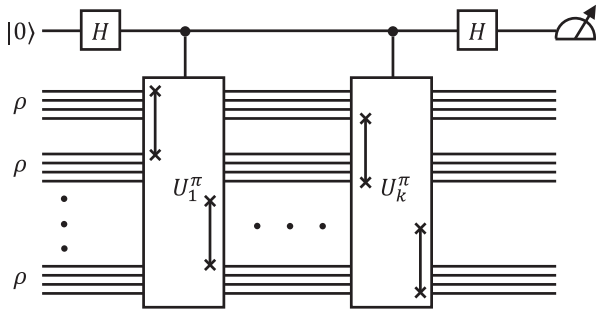

FIG. 2. Quantum circuit for measuring M_{2n}^{π}. Inputs of this algorithm are $2n$ identical copies of ρ and an ancilla qubit. The quantum gates in this circuit include Hadamard gates, labeled with H, and the control-U_i^π gate. The measurement of the ancilla qubit is in computational basis.

$$M_{2n}^{\pi} = \mathrm{tr}(O_{2n}^{\pi}\rho^{\otimes 2n}) = \frac{1}{2}\mathrm{tr}\left[\left(\bigotimes_{i=1}^{k} U_i^{\pi} + \mathrm{H.c.}\right)\rho^{\otimes 2n}\right]. \quad (4)$$

For T1-type parties, $U_i^\pi = \vec{\Pi}_i$, and for T2-type parties, $U_i^\pi = \overleftarrow{\Pi}_i$. Here, $\vec{\Pi}$ and $\overleftarrow{\Pi}$ are the cyclic permutation operators in different directions, satisfying $\vec{\Pi}|s_1, \ldots, s_{2n}\rangle = |s_{2n}, s_1, \ldots, s_{2n-1}\rangle$ and $\overleftarrow{\Pi}|s_1, \ldots, s_{2n}\rangle = |s_2, \ldots, s_{2n}, s_1\rangle$. For R1-type parties $U_i^\pi = \mathbb{S}_i^{(2n,1)} \otimes \mathbb{S}_i^{(2,3)} \otimes \cdots \otimes \mathbb{S}_i^{(2n-2,2n-1)}$ and for R2-type parties $U_i^\pi = \mathbb{S}_i^{(1,2)} \otimes \mathbb{S}_i^{(3,4)} \otimes \cdots \otimes \mathbb{S}_i^{(2n-1,2n)}$, where $\mathbb{S}^{(u,v)}$ is the SWAP operator acting on the uth and vth copies.

We leave the proofs of theorems in the Supplemental Material [29]. The special cases of partial transposed and realigned moments for a two-qubit system have been discussed in Refs. [38,39].

Borrowing the ideas from [14,39,40], by introducing an ancilla qubit, we can design a quantum circuit to measure M_{2n}^{π} based on the control-unitary operations; see Fig. 2. As the SWAP operators are the generators of the permutation group, all the control-unitary operators in this circuit can be decomposed into a polynomial number of the 3-qubit control-SWAP operators.

However, the simultaneous preparation of $2n$ identical copies of ρ is greatly challenging for state-of-the-art quantum devices. Fortunately, the recently developed techniques, shadow estimation [41,42] and randomized measurements [9,15,16], provide means to measure these moments by local (single-qubit) or global (multiqubit) single-copy operations. Practically speaking, global operations are still challenging, and local protocols are the ones commonly used in real experiments. Shadow estimation has a wide range of applications while inefficient in general. Randomized measurement has lower sample complexities, while it can only measure some specialized physical quantities. In Supplemental Material [29], we propose the measurement of the permutation moments using these two protocols and a hybrid one and analyze their sample complexities.

TABLE II. This table shows the best-known sample complexities of measuring $M_3^{(1,2)}$ and the complexities of protocols developed in Supplemental Material [29] to measure $M_4^{(2,3)}$. D is the dimension of the underlying Hilbert space. This table shows a nearly quadratic improvement in the local case.

	Global protocol	Local protocol
$M_3^{(1,2)}$	$O(D^{\frac{2}{3}})$ [45]	$O(D^2)$ [43]
$M_4^{(2,3)}$	$O(D^{\frac{1}{2}})$	$O(D^{1.187})$

In the bipartite scenario, $M_n^{(1,2)} = \mathrm{tr}\{[\mathcal{R}_{(1,2)}]^n\} = \mathrm{tr}[(\rho_{AB}^{T_A})^n]$ and $M_{2n}^{(2,3)}$ are key quantities that help to construct the weak-form PPT criteria [28,43,44] and the criteria proposed later in Eq. (7) and Eq. (8), respectively. The local randomized measurements scheme is not applicable for the measurement of $M_n^{(1,2)}$ [45]. The existing single-copy local protocol for measuring $M_n^{(1,2)}$ requires the shadow scheme, while, according to Theorem 1, the observables for measuring $M_{2n}^{(2,3)}$ have a simple form. Thus, $M_{2n}^{(2,3)}$ can be measured through the local randomized measurements protocol and have a much lower sample complexity. We list the sample complexities of measuring $M_3^{(1,2)}$ and $M_4^{(2,3)}$ in Table II.

To find the lower bound of $\|\mathcal{R}_\pi\| = \sum_i \lambda_i$ using these moments, one needs to solve an optimization problem. The original optimization problem is extremely hard to solve because we have an exponentially large number of λ_i. Adopting the Lagrange multiplier method, we can simplify the optimization to a problem of solving a set of polynomial equations.

Theorem 2: The minimum value of $\|\mathcal{R}_\pi\|$ given $M_2^\pi, \ldots, M_{2n}^\pi$ is reached when there are at most n nonzero λ_is. Thus, denote the solution of this problem to be $E_{2n}^\pi(\rho)$, it is equal to the solution of the following optimization problem,

$$\begin{aligned} \min_{q_1,\ldots,q_n\in\mathbb{N}} E_{2n}^{\pi}(\rho) &= q_1\lambda_1 + q_2\lambda_2 + \cdots + q_n\lambda_n \\ \text{s.t.} \sum_{i=1}^{n} q_i\lambda_i^2 &= M_2^\pi, \ldots, \sum_{i=1}^{n} q_i\lambda_i^{2n} = M_{2n}^\pi \\ q_1 + q_2 + \cdots + q_n &\le L, \end{aligned} \quad (5)$$

where L is the number of the singular values of $\mathcal{R}_\pi$ and q_i is the degeneracy of singular value λ_i.

As a special case, when we only know the value of M_2^π and M_4^π, the minimum of $\sum_i \lambda_i$ has an analytical form [46]:

$$E_4^{\pi}(\rho) = \sqrt{\frac{q(qM_2^\pi + U)}{q+1}} + \sqrt{\frac{M_2^\pi - U}{q+1}}, \quad (6)$$

where $q = \lfloor (M_2^\pi)^2/M_4^\pi \rfloor$ and $U = \sqrt{q(q+1)M_4^\pi - q(M_2^\pi)^2}$.

Now, we can formally represent the moment-based permutation criteria as

$$E_{2n}^{\pi}(\rho) \leq 1, \qquad \forall\ \pi \in \mathcal{S}_{2k}, \qquad n \in \mathbb{N} \tag{7}$$

for all separable k-partite state ρ. In fact, $E_{2n}^{\pi}(\cdot)$ may not necessarily be the function of ρ. Adopting the bipartite entanglement criterion introduced in Ref. [23], we get

$$E_{2n}^{(2,3)}(\rho_{AB} - \rho_A \otimes \rho_B) \leq \sqrt{(1-\mathrm{tr}\rho_A^2)(1-\mathrm{tr}\rho_B^2)} \tag{8}$$

for separable ρ_{AB}.

Bipartite entanglement detection.—Compared with existing entanglement detection schemes based on partial transposed moments [28,43,44], this framework is not only a direct generalization to multipartite entanglement, but also enhances the detection capability in the bipartite scenario. With the second and fourth moments only, Eq. (8) can detect 3×3-dimensional bound entanglement constructed using the unextendible product basis proposed in Ref. [47]. We leave the detailed discussion in the Supplemental Material [29].

The criterion of Eq. (8) also performs well in practical physical systems. We study the local bipartite entanglement dynamics in a quantum system evolved under a long-range XY Hamiltonian. Specifically, we choose a 10-qubit open boundary Ising model with the Hamiltonian of the form

$$H_{XY} = \sum_{i<j} J_{ij}(\hat{\sigma}_i^+ \hat{\sigma}_j^- + \hat{\sigma}_i^- \hat{\sigma}_j^+) + B_z \sum_i \hat{\sigma}_i^z, \tag{9}$$

where $\hat{\sigma}_i^z$, $\hat{\sigma}_i^+$, and $\hat{\sigma}_i^-$ are the spin-$\frac{1}{2}$ Pauli-Z, raising, and lowering operator acting on the ith qubit; $J_{ij} = (J_0/|i-j|^{\alpha})$ is the interaction strength following the power-law decay with J_0 and α set to be 420 s^{-1} and 1.24, respectively [9]; B_z stands for transverse field and is set to be 400 s^{-1}. This Hamiltonian has been realized in real physical systems [9,48] and has often served as the benchmark of detection capabilities of entanglement criteria [43,44].

The 10-qubit chain is divided into three parts, A, B, and C, where A and B constitute the local system we study, initialized to be $(1/\sqrt{2})(|0\rangle^{\otimes N_{AB}} + |1\rangle^{\otimes N_{AB}})$. C acts as the bath, which is initialized to be the tensor product of $|0\rangle$. We compare four implementable nonlinear criteria in investigating the entanglement dynamics of systems composed of A and B. The first two criteria are Eqs. (7) and (8), when setting $\pi = (2,3)$ and $n = 2$, labeled by $E_4^{(2,3)}$ and E_4^*, respectively. Others are the entropy criterion based on the comparison of the purities [1], labeled by P_2; and the weak-form PPT criterion based on $M_3^{(1,2)} = \mathrm{tr}[(\rho_{AB}^{T_A})^3]$ [28,44], labeled by P_3. We define four quantities to represent these criteria that satisfy that $E(\rho) > 0$ if and only if the entanglement is detected by the corresponding criterion.

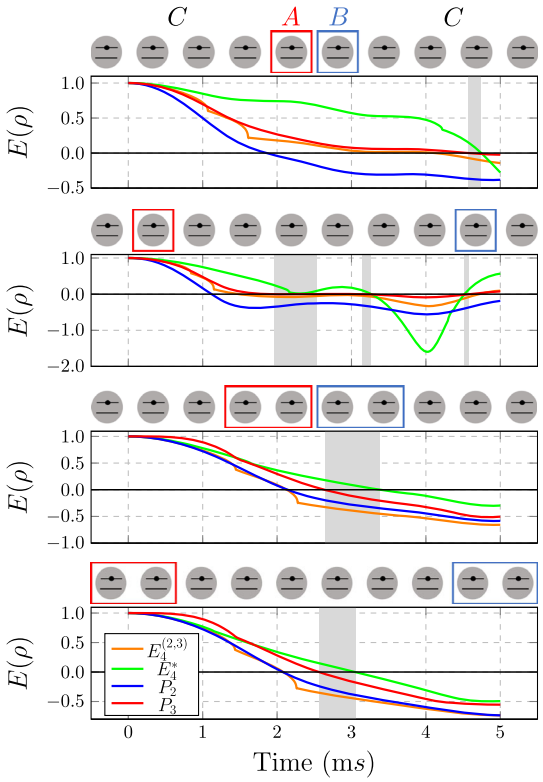

FIG. 3. Local entanglement decay in thermal system. The entanglement dynamics of the local systems A and B, which are marked by squares and initialized to be $|\psi(t=0)\rangle_{AB} = (1/\sqrt{2})(|0\rangle^{\otimes N_{AB}} + |1\rangle^{\otimes N_{AB}})$. Qubits without squares are initialized to be the tensor product of $|0\rangle\langle 0|$, act as part C. The entanglement of AB is detected when the value is above zero for each criterion. The gray areas represent the time periods in which the entanglement can only be detected by the E_4^* criterion.

The numerical simulation results [49] are shown in Fig. 3. One could find that the moment-based permutation criteria, especially E_4^*, have an obvious advantage since they detect entanglement while all others fail in various time periods and different choices of A and B.

In addition to the strong detection capability, the key quantities in this framework, $E_{2n}^{\pi}(\rho)$, have clear mathematical meaning as they give the lower bounds of the permutation norms. The permutation norms, including entanglement negativity, can be treated as entanglement measures. We thus conjecture that these quantities can also be used as entanglement measures. In Supplemental Material [29], we support this conjecture by showing that $E_4^{(2,3)}(\rho)$ can witness the entanglement scaling transition in a quantum dynamical phase transition [6,50–52] and the entanglement rainbow structure for the eigenstates of a thermal Hamiltonian [2,53,54].

Multipartite entanglement detection.—Another advantage of our framework lies in multipartite entanglement detection. There exist multipartite entangled states that are separable in any bipartition and thus cannot be detected by

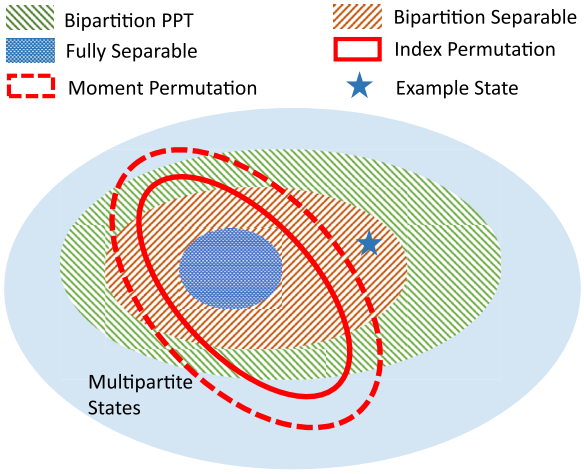

FIG. 4. Illustration of different sets of detectable states. Bipartition PPT, PPT in any bipartition; Bipartition Separable, separable in any bipartition; Fully Separable, $\sum_i p_i \rho_1^i \otimes \cdots \otimes \rho_k^i$; Index Permutation, states that cannot be detected by an index permutation criterion other than the bipartite partial transposition; Moment Permutation, states that cannot be detected using finite numbers of permutation moments; Example State, a state that is separable in any bipartition while being detectable by a moment-based permutation criterion. When the number of moments increases, the dashed red circle will approach the solid red circle.

any criteria extended from the bipartite case [55], including the PPT and CCNR criteria. Theorem 2 provides us new means to design practical entanglement criteria for these states. We depict the sets of detectable multipartite entangled states of different criteria in Fig. 4.

An important example is also based on the unextendible product basis [47]. Consider a three-qubit system and define four product pure states

$$\{|\psi\rangle_i\}_{i=1}^4 = \{|0,1,+\rangle, |1,+,0\rangle, |+,0,1\rangle, |-,-,-\rangle\}, \quad (10)$$

where $|\pm\rangle = (|0\rangle \pm |1\rangle)/\sqrt{2}$. It has been proved that the state

$$\rho = \frac{1}{4}\left(\mathbb{I}_8 - \sum_{i=1}^{4} |\psi_i\rangle\langle\psi_i|\right) \quad (11)$$

is separable in any bipartition and thus its detection needs a new kind of moment-based permutation criterion other than PPT and CCNR. We find that when setting $\pi = \binom{1,2,3,4,5,6}{1,3,2,4,5,6}$, realigning the first two parties and keeping the third party unchanged, the entanglement of this state can be detected using $E_8^{\pi}(\rho)$, which only requires 4 orders of moments. We leave some details of calculating $E_8^{\pi}(\rho)$ in Supplemental Material.

For multipartite quantum systems, entanglement can have a rather complex entanglement structure [56]. At the same time, the tools for detecting entanglement structure are quite restrictive [57]. In Supplemental Material [29], we show that our framework can also be generalized to detect the multipartite entanglement structure.

Outlook.—The techniques we developed in this Letter, including the moment measurements and bounding the lower-order moment using the higher-order moments, have many potential applications, like positive map entanglement detection [11] and trace distance estimation. Furthermore, it is also interesting to investigate how to generalize the framework to entanglement detection in continuous variable systems [58].

We thank Junjie Chen, Zhaohui Wei, and Xiaodong Yu for valuable discussions. This work was supported by the National Natural Science Foundation of China Grants No. 12174216 and No. 11875173 and the National Key Research and Development Program of China Grants No. 2019QY0702 and No. 2017YFA0303903.

*Corresponding author.
xma@tsinghua.edu.cn

[1] R. Horodecki, P. Horodecki, M. Horodecki, and K. Horodecki, Rev. Mod. Phys. **81**, 865 (2009).
[2] M. Ueda, Nat. Rev. Phys. **2**, 669 (2020).
[3] A. M. Kaufman, M. E. Tai, A. Lukin, M. Rispoli, R. Schittko, P. M. Preiss, and M. Greiner, Science **353**, 794 (2016).
[4] N. Laflorencie, Phys. Rep. **646**, 1 (2016).
[5] T. Nishioka, Rev. Mod. Phys. **90**, 035007 (2018).
[6] D. A. Abanin, E. Altman, I. Bloch, and M. Serbyn, Rev. Mod. Phys. **91**, 021001 (2019).
[7] L. Amico, R. Fazio, A. Osterloh, and V. Vedral, Rev. Mod. Phys. **80**, 517 (2008).
[8] L. Gurvits, in *Proceedings of the Thirty-Fifth Annual ACM Symposium on Theory of Computing* (Association for Computing Machinery, New York, NY, USA, 2003), STOC '03, pp. 10–19, ISBN 1581136749, 10.1145/780542.780545.
[9] T. Brydges, A. Elben, P. Jurcevic, B. Vermersch, C. Maier, B. P. Lanyon, P. Zoller, R. Blatt, and C. F. Roos, Science **364**, 260 (2019).
[10] C. Kokail, B. Sundar, T. V. Zache, A. Elben, B. Vermersch, M. Dalmonte, R. van Bijnen, and P. Zoller, Phys. Rev. Lett. **127**, 170501 (2021).
[11] O. Gühne and G. Tóth, Phys. Rep. **474**, 1 (2009).
[12] Y. Zhang, Y. Tang, Y. Zhou, and X. Ma, Phys. Rev. A **103**, 052426 (2021).
[13] J. Preskill, Quantum **2**, 79 (2018).
[14] A. K. Ekert, C. M. Alves, D. K. L. Oi, M. Horodecki, P. Horodecki, and L. C. Kwek, Phys. Rev. Lett. **88**, 217901 (2002).
[15] S. J. van Enk and C. W. J. Beenakker, Phys. Rev. Lett. **108**, 110503 (2012).
[16] A. Elben, B. Vermersch, C. F. Roos, and P. Zoller, Phys. Rev. A **99**, 052323 (2019).
[17] G. Smith, J. A. Smolin, X. Yuan, Q. Zhao, D. Girolami, and X. Ma, arXiv:1707.09928.
[18] P. Horodecki, Phys. Rev. Lett. **90**, 167901 (2003).

[19] S. Imai, N. Wyderka, A. Ketterer, and O. Gühne, Phys. Rev. Lett. **126**, 150501 (2021).
[20] J. L. Beckey, N. Gigena, P. J. Coles, and M. Cerezo, Phys. Rev. Lett. **127**, 140501 (2021).
[21] A. Ketterer, S. Imai, N. Wyderka, and O. Gühne, Phys. Rev. A **106**, L010402 (2022).
[22] M. Horodecki, P. Horodecki, and R. Horodecki, Open Syst. Inf. Dyn. **13**, 103 (2006).
[23] C.-J. Zhang, Y.-S. Zhang, S. Zhang, and G.-C. Guo, Phys. Rev. A **77**, 060301(R) (2008).
[24] A. Peres, Phys. Rev. Lett. **77**, 1413 (1996).
[25] K. Chen and L.-A. Wu, Quantum Info. Comput. **3**, 193 (2003).
[26] J. Haah, A. W. Harrow, Z. Ji, X. Wu, and N. Yu, IEEE Trans. Inf. Theory **63**, 5628 (2017),
[27] J. Gray, L. Banchi, A. Bayat, and S. Bose, Phys. Rev. Lett. **121**, 150503 (2018).
[28] X.-D. Yu, S. Imai, and O. Gühne, Phys. Rev. Lett. **127**, 060504 (2021).
[29] See Supplemental Material at http://link.aps.org/supplemental/10.1103/PhysRevLett.129.260501 for proofs of main theorems, measurement protocols and statistical analysis of the permutation moments, and details of physical simulations, which includes Refs. [30–37].
[30] C. J. Wood, J. D. Biamonte, and D. G. Cory, Quantum Inf. Comput. **15**, 759 (2015).
[31] Y. Gu, Moments of random matrices and weingarten functions, Ph.D. thesis, 2013.
[32] D. A. Roberts and B. Yoshida, J. High Energy Phys. 04 (2017) 121.
[33] H. Zhu, Phys. Rev. A **96**, 062336 (2017).
[34] R. A. Horn, R. A. Horn, and C. R. Johnson, *Topics in Matrix Analysis* (Cambridge University Press, Cambridge, England, 1994).
[35] M. Li, J. Wang, S. Shen, Z. Chen, and S.-M. Fei, Sci. Rep. **7**, 17274 (2017).
[36] Z. Liu, P. Zeng, Y. Zhou, and M. Gu, Phys. Rev. A **105**, 022407 (2022).
[37] A. Rath, C. Branciard, A. Minguzzi, and B. Vermersch, Phys. Rev. Lett. **127**, 260501 (2021).
[38] H. A. Carteret, Phys. Rev. Lett. **94**, 040502 (2005).
[39] J. Cai and W. Song, Phys. Rev. Lett. **101**, 190503 (2008).
[40] E. Knill and R. Laflamme, Phys. Rev. Lett. **81**, 5672 (1998).
[41] S. Aaronson, SIAM J. Comput. **49**, STOC18 (2019).
[42] H.-Y. Huang, R. Kueng, and J. Preskill, Nat. Phys. **16**, 1050 (2020).
[43] A. Elben, R. Kueng, H. Y. R. Huang, R. van Bijnen, C. Kokail, M. Dalmonte, P. Calabrese, B. Kraus, J. Preskill, P. Zoller *et al.*, Phys. Rev. Lett. **125**, 200501 (2020).
[44] A. Neven, J. Carrasco, V. Vitale, C. Kokail, A. Elben, M. Dalmonte, P. Calabrese, P. Zoller, B. Vermersch, R. Kueng *et al.*, npj Quantum Inf. **7**, 152 (2021).
[45] Y. Zhou, P. Zeng, and Z. Liu, Phys. Rev. Lett. **125**, 200502 (2020).
[46] D. W. Berry and B. C. Sanders, J. Phys. A **36**, 12255 (2003).
[47] C. H. Bennett, D. P. DiVincenzo, T. Mor, P. W. Shor, J. A. Smolin, and B. M. Terhal, Phys. Rev. Lett. **82**, 5385 (1999).
[48] P. Jurcevic, B. P. Lanyon, P. Hauke, C. Hempel, P. Zoller, R. Blatt, and C. F. Roos, Nature (London) **511**, 202 (2014).
[49] J. Johansson, P. Nation, and F. Nori, Comput. Phys. Commun. **183**, 1760 (2012).
[50] M. Serbyn, Z. Papić, and D. A. Abanin, Phys. Rev. Lett. **111**, 127201 (2013).
[51] J. Smith, A. Lee, P. Richerme, B. Neyenhuis, P. W. Hess, P. Hauke, M. Heyl, D. A. Huse, and C. Monroe, Nat. Phys. **12**, 907 (2016).
[52] Y.-L. Wu and S. Das Sarma, Phys. Rev. A **93**, 022332 (2016).
[53] H. Kim, T. N. Ikeda, and D. A. Huse, Phys. Rev. E **90**, 052105 (2014).
[54] J. S. Cotler, D. K. Mark, H.-Y. Huang, F. Hernandez, J. Choi, A. L. Shaw, M. Endres, and S. Choi, arXiv:2103.03536.
[55] B. Jungnitsch, T. Moroder, and O. Gühne, Phys. Rev. Lett. **106**, 190502 (2011).
[56] H. Lu, Q. Zhao, Z.-D. Li, X.-F. Yin, X. Yuan, J.-C. Hung, L.-K. Chen, L. Li, N.-L. Liu, C.-Z. Peng *et al.*, Phys. Rev. X **8**, 021072 (2018).
[57] Z. Ren, W. Li, A. Smerzi, and M. Gessner, Phys. Rev. Lett. **126**, 080502 (2021).
[58] C. Zhang, S. Yu, Q. Chen, and C. H. Oh, Phys. Rev. Lett. **111**, 190501 (2013).